International Research Journal of Engineering and Technology (IRJET) e-ISSN: 2395 -0056
Volume: 02 Issue: 07 | Oct-2015 www.irjet.net p-ISSN: 2395-0072

Design of Shunt Active Power Filter by using An Advanced Current Control Strategy

K.Sailaja[1], M.Jyosthna Bai[2]

[1] *PG Scholar, Department of EEE, JNTU Anantapur, Andhra Pradesh, India*
[2] *PG Scholar, Department of EEE, JNTU Anantapur, Andhra Pradesh, India*

Abstract - To enhance the performance of shunt Active Power Filter(APF),an advanced current control strategy is used. The control scheme requires two sensors at the supply side and there is no need of a harmonic detector. With the help of Proportional-Integral (PI) and Vector Proportional –Integral(VPI) controllers, an effective harmonic compensation method is developed to make the supply currents sinusoidal. The simplified control scheme and improved accuracy of the APF is possible with the absence of harmonic detector. With the use of minimized current sensors and Four-Switch Three-Phase Inverter(FSTPI), cost of APF becomes low.

***Keywords*— Shunt Active Power Filter, PI plus VPI controllers, non linear loads, harmonics, four switch three phase inverter, control loops, phase locked loop.**

1. INTRODUCTION

Huge amounts of harmonic currents injects into the distribution system due to the increasing usage of non-linear loads like electric arc welders, switching power supplies and speed drives. These harmonic currents are the reason for voltage distortion, electronic equipment operational failures and high power losses etc. Because of these problems harmonic restriction standards demand at to maintain the harmonic currents injected into the networks must be below the specified values[1],[2]. There are two main solutions to meet the restriction standards such as LC Passive filters and Active Power Filters(APF's)[3]-[5].Shunt Active Power Filters are the flexible solution for the harmonic current compensation.

Shunt active power filter

A Shunt active power filter generates a harmonic current that must have equal magnitude but opposite phase to compensate the current harmonics that means the phase is shifted by 180^0. Active Filter cancels the harmonics present in load current, and source current will remain sinusoidal and in phase with neutral voltage.

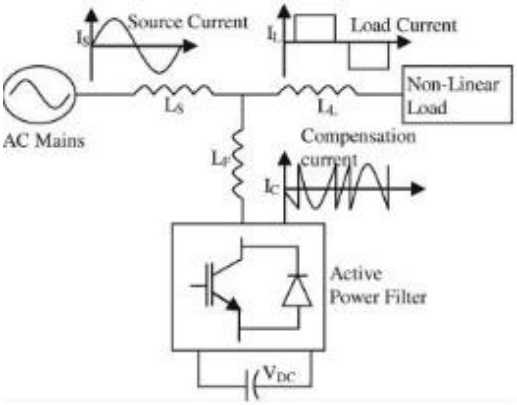

Fig.1 Compensation characteristics of a shunt active power filter.

2. CONTROL STRATEGY

To get the accuracy of the APF and to simplify the control scheme, an advanced control strategy is designed as shown in Fig.2. without predicting the load current($i_{L,abc}$) and filter current ($i_{F,abc}$), a control scheme is designed by using only the supply current ($i_{Sa}$and i_{Sb}).

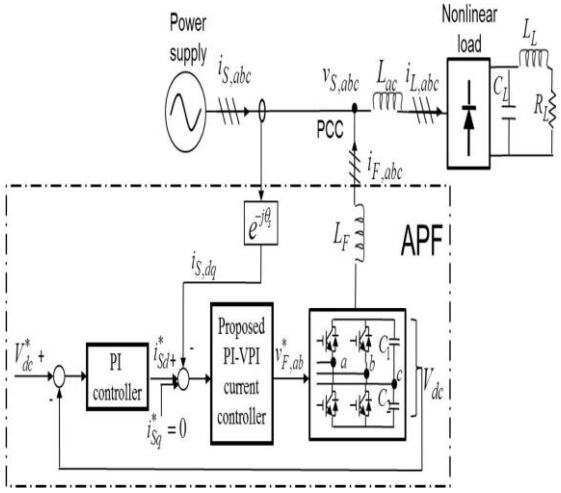

Fig. 2 Structure of the PI-Vector PI control scheme for three-phase shunt APF.

The control scheme is implemented with only two loops with the harmonic detector absence. One is the outer voltage control loop and another is the inner current control loop. The voltage control loop keeps the DC-link voltage of the APF constant with a PI controller, through which the APF can deal the load variations. In the fundamental reference frame(i^*_{sd}), the output of the voltage control loop is the reference active current. The reference reactive current (i^*_{sd}) is said to zero, which shows the reactive power of the power supply is to be zero. By using the PI plus VPI controllers, the current control loop is used to regulate the supply current in the fundamental reference frame loop($i_{s,dq}$). The output of the current control loops becomes the control signal ($v^*_{F,ab}$) to the four switch APF. The performance of the APF depends only on the current controller since current control is executed in the absence of harmonic detector.

Current control scheme using PI plus Vector PI (VPI)controllers

By using a PI controller only, it is almost difficult to force the supply currents be sinusoidal in the APF system. The Supply currents are indirectly controlled by regulating a non-sinusoidal filter currents. Due to the bandwidth limitation, PI Controller is not able to totally regulate the high frequency signals. Harmonic currents are the examples of the high frequency signals. So only PI current controller is unable to achieve the required control target of APF . Multiple resonant controllers have high gains tuned at harmonic frequencies are used to regulate the supply currents to be sinusoidal.

The Transfer Function of multiple proportional resonant controllers is given as

$$G_{PR} = \sum_{h=1,5,7,11,13} K_{ph} + \frac{2K_{rh}s}{s^2+(h\omega_s)^2} \quad (1)$$

where K_{ph} and K_{rh} are the proportional and resonant gains of the resonant controller, respectively, h is the order of harmonic currents, and w_s is the fundamental frequency of the supply voltage.

As shown in equation (1), each controller has to regulate only one harmonic component so the complexity and computational burden will be increased in case of large number of harmonic currents are to be compensated. In the fundamental reference frame each pair of $h = 6n \pm 1$ harmonic currents behave as $h = 6n$ harmonic currents. So a resonant controller tuned at $h = 6n$ multiples of w_s is possible in the reference frame regulating a pair of $h = 6n \pm 1$ harmonic currents.

The transfer function of resonant controllers is given as

$$G_{PI-R} = K_{p1} + \frac{K_{i1}}{s} + \sum_{h=6,12,18} K_{ph} + \frac{2K_{rh}s}{s^2+(h\omega_s)^2} \quad (2)$$

where K_{p1} and K_{i1} are the proportional and integrator gains of the PI controller respectively, $h = 6n$ is the order of harmonics in the fundamental reference frame with $n = 1, 2, 3 \ldots$.

In equation (2),PI controller is used to regulate the fundamental currents and resonant controllers are aimed to control the harmonic currents. If the high-order harmonics are to be compensated, we must take two factors in to account, time delay caused by the effect of APF and digital implementation. Then the transfer function of the PI-R controller will becomes

$$G_{PI-R} = K_{p1} + \frac{K_{i1}}{s} + \sum_{h=6,12,18} K_{ph} + 2K_{rh}\frac{s\cos(h\omega_s NT_s) - h\omega_s \sin(h\omega_s NT_s)}{s^2+(h\omega_s)^2} \quad (3)$$

where N is the number of samples and T_s is the sampling period. Best result obtained when $N = 2$.

In equation (3), the compensation method considers the delay time and neglect the effect of APF. So that the stability margins get reduced and undesired peaks appear in the frequency response when the order of the compensated harmonics as in the fig (3). To overcome these problems, the solution of the resonant controller is VPI controller.

The Transfer Function of the Vector PI controller is given as

$$G_{VPI} = \sum_{h=6,12,18} 2\frac{K_{ph}s^2 + K_{rh}s}{s^2+(h\omega_s)^2} \quad (4)$$

The VPI controller cancels the coupling term $1/(sL_F + R_F)$ by selecting the $K_{rh} = K_{ph}R_F/L_F$ where L_F and R_F are the inductance and resistance of the inductor. Using this advantage ,the VPI controller removes the peaks in the closed-loop response without delay compensation. Hence the resonant controllers are replaced with VPI controllers.

The Transfer Function of the PI-VPI controllers is given as

$$G_{PI-VPI} = K_{p1} + \frac{K_{i1}}{s} + \sum_{h=6,\ldots,30} 2\frac{K_{ph}s^2 + K_{rh}s}{s^2+(h\omega_s)^2} \quad (5)$$

To investigate the characteristics of the PI-VPI controllers over the PI controllers, fig.(4) shows open-loop Bode diagram for the PI and VPI controllers given in equation(5) for the case of $h = 6n$, $n = 1 \ldots 5$, $\omega_s = 2\pi 60$ rad/s, $K_{ph} = 1$, and $K_{rh} = K_{ph}R_F/L_F$ .At low frequencies (less than 20 Hz), the gains of the PI and VPI controllers are high, but at high resonant frequencies ($6\omega_s$, $12\omega_s$, $18\omega_s$, $24\omega_s$, and $30\omega_s$), the PI controller gain is reduced while the VPI controller produces very high gains for getting

zero steady–state errors in the harmonic current compensation. The PI-VPI controller removes the undesired peaks through the pole-zero cancellation capacity with the L_F inductor.

The L_F inductor model is defined by equation (6) and the closed-loop Transfer Function of the VPI current control is given in equation(7).

$$G_{L_F} = \frac{1}{sL_F + R_F} \quad (6)$$

Fig.3 shows the Bode diagram of the closed-loop Transfer Function for the VPI controller, PI-R controller with $h = 6n$, $n = 1 \ldots 5$, $K_{ph} = 1$, and $K_{rh} = K_{ph}R_F/L_F$. The VPI controller provides zero phase shift and unity gain for all the selected resonant frequencies. Hence we can say that VPI controllers improves the accuracy and stability margins of the current controller significantly.

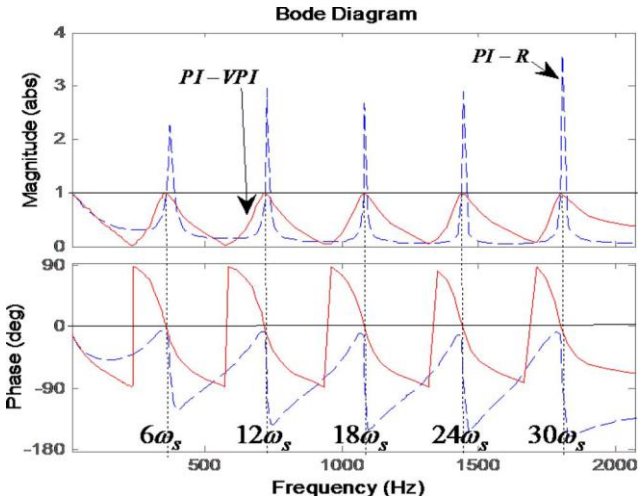

Fig. 3 Closed-loop Bode diagrams of the PI-VPI and PI-R controller.

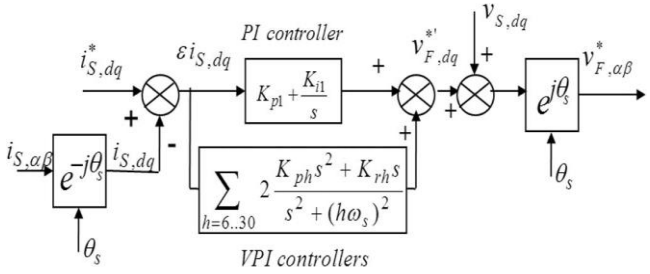

Fig.4 Block diagram of the proposed current control scheme.

The PI-VPI current controller scheme is shown in figure(4). The measured supply current $i_{S,\alpha\beta}$ must be transformed from stationary to the fundamental reference frame $i_{S,dq}$ since the VPI current controller is designed in fundamental reference frame. The VPI current controller is executed to regulate this current follow the reference $i^*_{S,dq}$. The output of the controller $v^*_{F,dq}$ and feed forward supply voltage term $v_{S,dq}$ are added together and transformed to stationary reference frame with an inverse location transformation to obtain command voltage nothing but the control signal of APF $v^*_{F,\alpha\beta}$

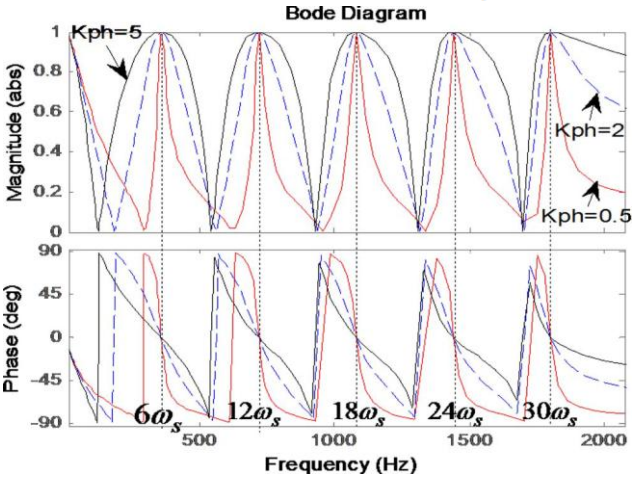

Fig. 5 Closed-loop Bode diagrams of the VPI controllers with K_{ph} = 0.5, K_{ph} = 2, and K_{ph} = 5.

Current controller design:

The closed-loop transfer function of the PI-VPI current controller shown in equation (7) is analyzed to design and investigate the gains for the PI-VPI controller. The closed –loop transfer function of the PI-VPI controller becomes as shown in the equation (8) after selecting the resonant gain as $K_{rh} = K_{ph}R_F/L_F$ and $K_{i1} = K_{p1}R_F/L_F$. K_{ph} and K_{p1} are gains to be tuned. K_{p1} is said to be constant andK_{ph} is varied to determine the control performance of the PI controller with the values of K_{ph} = 0.5, K_{ph} = 2, and K_{ph} = 5, the Bode diagram is as shown in figure 3.5. VPI controller provides unity gain and zero phase-shift regardless of the K_{ph} values at selected resonant frequencies. The VPI controller is selective and obtain better steady state performance if the K_{ph} is a small value. i.e. K_{ph}<1 but it should not too less since it may destroy the dynamic response of the APF.

$$G_C = \frac{G_{PI-VPI}\,G_{L_F}}{1+G_{PI-VPI}\,G_{L_F}}$$

$$= \sum_{h=6,\ldots,30} \frac{(K_{p1}+2K_{ph})s^2+(K_{i1}+2K_{rh})s^2+K_{p1}(h\omega_s)^2s+K_{i1}(h\omega_s)^2}{L_Fs^4+(K_{p1}+2K_{ph}+R_F)s^3+(K_{i1}+2K_{rh}+L_F(h\omega_s)^2)s^2+(R_F+K_{p1})(h\omega_s)^2s+K_{i1}(h\omega_s)^2} \quad (7)$$

$$G_C = \sum_{h=6,\ldots,30} \frac{(K_{p1}L_F+2K_{ph})s^3+2K_{ph}K_{p1}s+K_{p1}L_F(h\omega_s)^2}{L_Fs^3+(K_{p1}L_F+4K_{ph})s^2+(2K_{ph}K_{p1}+L_F(h\omega_s)^2)s+K_{p1}L_F(h\omega_s)^2} \quad (8)$$

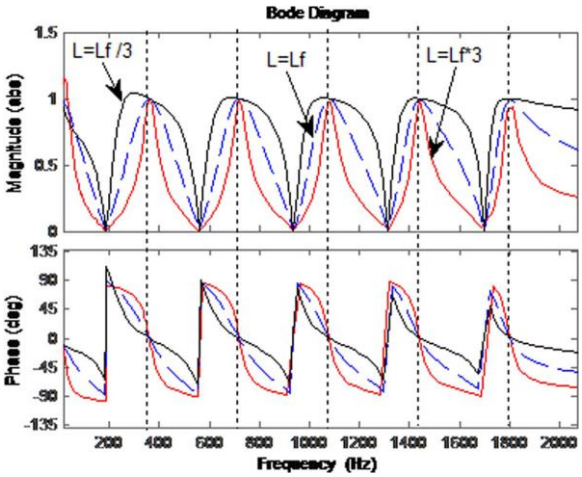

Fig.6 Closed-loop Bode diagrams of the VPI controllers with variation of the inductor parameters.

The gains of the controller obtained from the design process kept constant and inductor parameters changed in the operation period. The inductor parameters does not have any effect on the steady-state performance and stability of the APF.

Discrete-time implementation of the VPI(Vector PI) controllers

To realize the digital controller the important step is discretisation. Discretisation transfers the controller to discrete-time type from continuous time type to be implemented with digital signal processors and microcontrollers.

To achieve the accurate resonant code placement, the transfer function of VPI controller is given in Z-domain as shown below.

$$G_{VPI}(z) = \frac{K_{ph}+(K_{rh}T_s-2K_{ph})z^{-1}-(K_{rh}T_s-K_{ph})z^{-2}}{1-2\cos(h\omega_s T_s)z^{-1}+z^{-2}} \quad (9)$$

where *z* is the shift operator.

The cosine function in the above equation takes the large time calculation so it can be changed by using taylor series as given in equation (10)

$$\cos(h\omega_s T_s) = 1 - \frac{(h\omega_s T_s)^2}{2} + \frac{(h\omega_s T_s)^4}{24} + \frac{(h\omega_s T_s)^6}{720} \quad (10)$$

The fourth order approximation is used for the replacing cosine function in equation (9). Then the transfer function can be written as

$$G_{VPI}(z) = \frac{K_{ph}+(K_{rh}T_s-2K_{ph})z^{-1}-(K_{rh}T_s-K_{ph})z^{-2}}{1-2\left(1-\frac{(h\omega_s T_s)^2}{2}+\frac{(h\omega_s T_s)^4}{24}\right)z^{-1}+z^{-2}} \quad (11)$$

3. DESCRIPTION OF THE WHOLE CONTROL STRATEGY

The block diagram of the whole PI-VPI control strategy is shown in figure7. The control scheme has two loops: Supply current control loop and The DC-Link voltage control loop. Here Phase-Locked Loop(PLL) is used to track the supply voltage phase

Dc-link voltage control loop

The DC-link voltage of the shunt APF is kept constant through a PI controller and the output is the reference active current of the fundamental reference frame which is given as

$$i^*_{sd} = (K_{pdc} + \frac{K_{idc}}{s})(V^*_{dc} - V_{dc}) \quad (12)$$

Where K_{pdc} and K_{idc} are the proportional and integrator gains of the PI controller, respectively, and v^*_{dc} and V_{dc} are reference and measured dc-link voltages of the APF, respectively.

The four-switch APF needs higher DC-link voltage (v^*_{dc}) has since it has only two legs compared to the six-switch APF as shown in table(1). A Low Pass Filter(LPF) is used to eliminate the ripples in the DC-Link voltage that helps in smoothing the reference current i^*_{sd}. The DC-link voltage in the VPI control scheme helps in proper operation of the APF and deal with the load variations. The shunt APF respond against load variations without the measurement of load current.

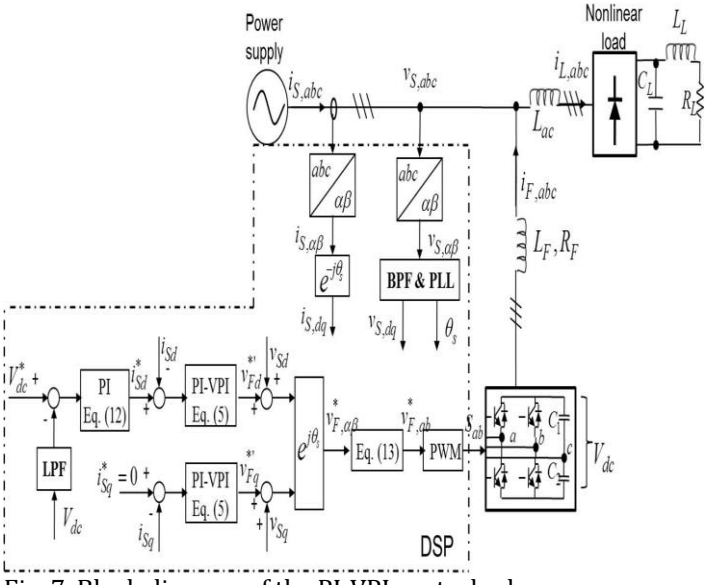

Fig. 7 Block diagram of the PI-VPI control scheme.

TABLE -1
SYSTEM PARAMETERS

Supply voltage RMS line-line	127V
Supply frequency	60Hz
5th harmonic supply voltage	10% of the fundamental component
7th harmonic supply voltage	5% of the fundamental component
DC-link reference voltage for the six-switch APF V^*_{dc}	260V
DC-link reference voltage for the four-switch APF V^*_{dc}	420V
DC-link capacitor for four switch APF C1=C2	1000μF
DC-link capacitor for six-switch APF C=C1+C2	2000μF
Filter Resistance R_F	0.05 ohms
Filter Inductance L_F	2mH
Nonlinear RLC load	$R_{L(min)}$=12.5ohm, $R_{L(max)}$ =20ohm L_L=1mH C_L =2200μF

Supply current control loop

This loop regulates the supply current by means of the proposed current control scheme shown in Fig. 6. The reference active current i^*_{sd} is the output of the dc-link voltage control loop given in equation (13), while the reference reactive current i^*_{sq} is simply set to be zero. Consequently, the reactive power caused by loads can be fully compensated by the APF, and also unity power factor condition is achieved at the supply side.

Control signal computation for the four-switch APF

The traditional three-phase VSI is commonly used to implement an APF. In this paper, in order to accomplish a low cost APF topology, the four-switch APF is introduced by replacing the traditional three-phase VSI with the FSTPI with- out degrading the performance of the proposed control strategy.

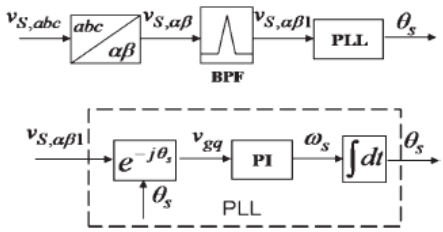

Fig. 8 Block diagram of the improved PLL.

The control signals of the Four-Switch APF are gives as

$$V^*_{Fa} = \sqrt{\frac{3}{2}} V^*_{F\alpha} + \sqrt{\frac{1}{2}} V^*_{F\beta}$$

$$V^*_{Fb} = \sqrt{2} V^*_{F\beta} \qquad (13)$$

Where v^*_{Fa} and v^*_{Fb} are the control signals for leg a and b of the four-switch APF respectively.

Supply voltage PLL(Phase-Locked Loop)

The phase of the supply voltage is tracked with this Phase locked loop. Supply voltage basically contains harmonic components in practical distribution system which affect the accuracy of the PLL. A Band Pass Filter(BPF) is used to overcome this problem which is tuned at fundamental frequency of supply voltage to remove the harmonics present in supply voltage . a small time delay may occur in the PLL even though BPF is used ,but it can be negligible because PLL operates at steady state condition before APF is on.

4.RESULTS

Simulation diagram

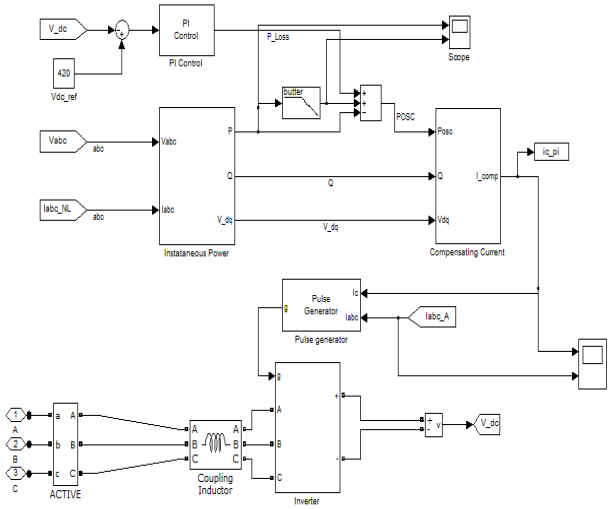

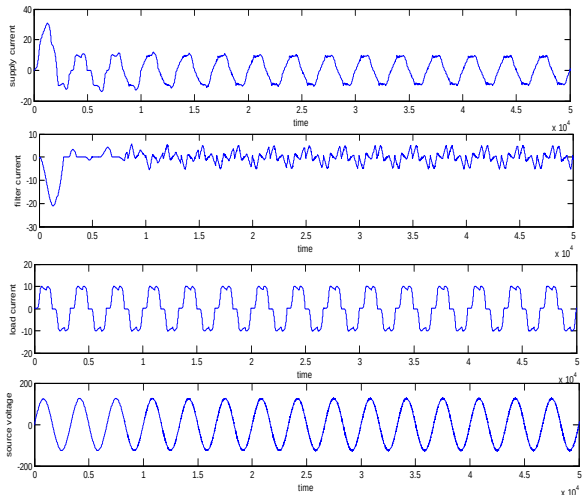

Fig.9 Steady state response of PI-Vector PI control scheme

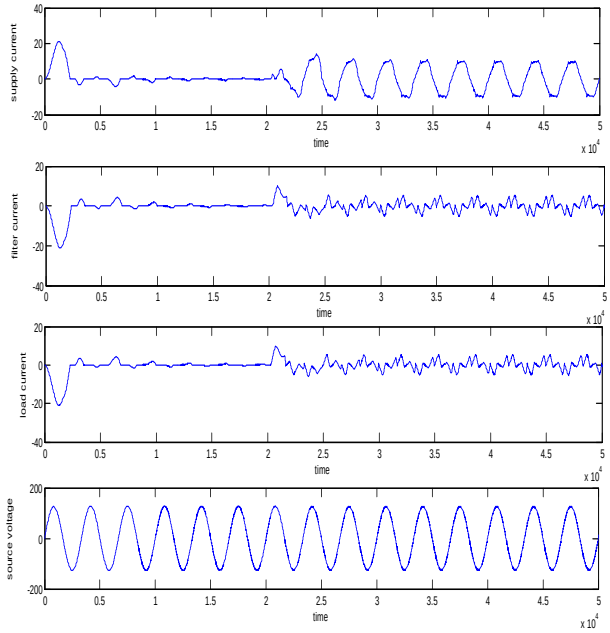

Fig.10 dynamic response of PI-Vector PI control scheme

Extension results

A 9 MW wind farm consisting of six 1.5 MW wind turbines connected to a 25 kV distribution system exports power to a 120 kV grid through a 30 km, 25 kV feeder is placed in place of grid in the simulation diagram of PI-VPI control system and got the result as shown bellow.

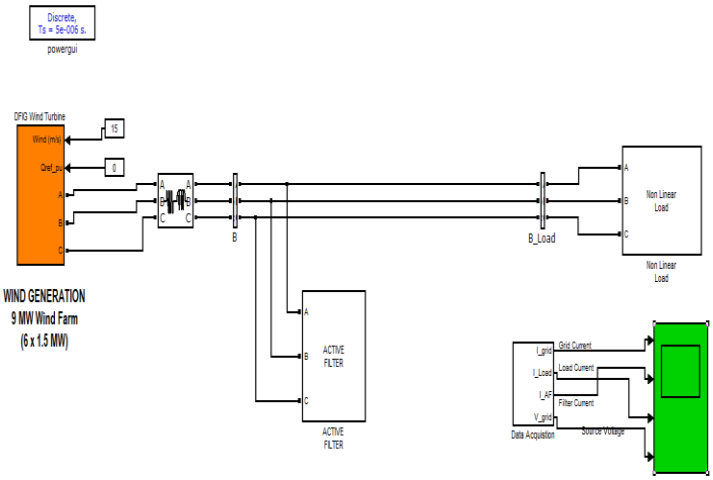

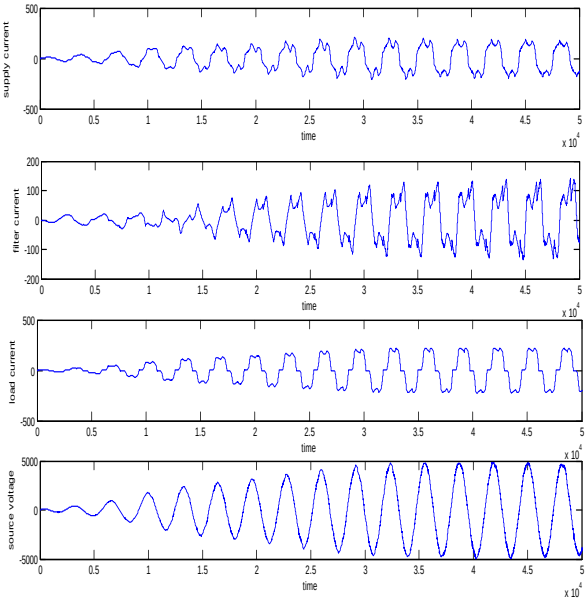

Fig.11 steady state response of PI-VPI control scheme with wind farm.

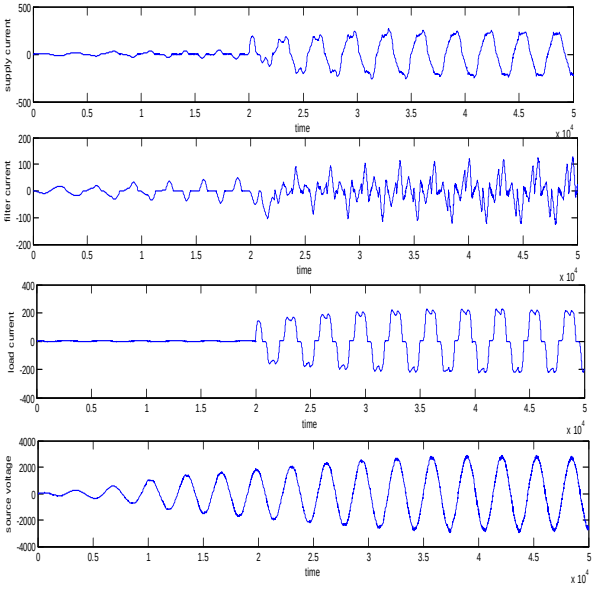

Fig.12 dynamic response of PI-VPI control scheme with wind farm

CONCLUSION

An advanced current control strategy for the three-phase shunt APF was designed. The effectiveness of the PI-VPI control strategy was verified, where the control strategy presented the good steady-state performance with nonlinear RLC and RL loads and also good dynamic response against the load variations. The supply current is almost sinusoidal and in-phase with the supply voltage even in the distorted voltage conditions.

Results verified that the faster transient responses and notches free steady-state performance of the supply current in the absence of harmonic detector. And also confirmed that Four-Switch Three-Phase Inverter(FSTPI) is used to implement the Active Power Filter(APF) without any degradation in the Active Power Filter performance.

REFERENCES

[1] Recommended Practice for Harmonic Control in Electric Power Systems,IEEE Std. 519-1992, 1992.
[2] Limits for Harmonic Current Emission, IEC 61000-3-2, 2001.
[3] H. Akagi, "New trends in active filters for power conditioning," IEEETrans. Ind. Appl., vol. 32, no. 2, pp. 1312–1332, Nov./Dec. 1996.
[4] F. Z. Peng, "Application issues of active power filters," IEEE Ind. Appl.Mag., vol. 4, no. 5, pp. 21–30, Sep./Oct. 1998.
[5] H. Akagi, E. H. Watanabe, and M. Aredes, Instantaneous Power Theory and Applications to Power Conditioning, M. E. El-Hawari, Ed.New York: Wiley, 2007.
[6] S. Buso, L. Malesani, and P. Mattavelli, "Comparison of current control techniques for active filters applications," IEEE Trans. Ind. Electron., vol. 45, no. 5, pp. 722–729, Oct. 1998.
[7] L.Malesani, P. Mattavelli, and S. Buso, "Robust dead-beat current control for PWM rectifiers and active filters," IEEE Trans. Ind. Appl., vol. 35,no. 3, pp. 613–620, May/Jun. 1999.